Roll Dynamic Response of an Articulated Vehicle carrying liquids

Jafari[1], Sh. Azadi[2] , M.Samadian[3,*]

1 Associate professor, 2.Asistant professor, 3.P.h.D Student. Mechanical Department, Khaje Nasir University of Technology, Tehran,Iran.

Abstract

The directional response and roll stability characteristics of a partly filled tractor semi-trailer vehicle, with cylindricaltank, are investigated in various maneuvers. The dynamic interaction of liquid cargo with the tractor semi-trailervehicle is also evaluated by integrating a dynamic slosh model of the partly filled tank with five-degrees-of-freedom ofa tractor semi-trailer tank model. The dynamic fluid slosh within the tank is modeled using three-dimensional Navier-Stokes equations, coupled with volume-of-fluid equations and analysed using the FLUENT software. The coupledtank-vehicle model is subsequently analysed to determine the roll stability characteristics for different maneuvers. Theresults showed the interaction of fluid slosh with vehicle's dynamic. Another findings of this investigation also revealed that the roll stability of a tractor semi-trailer tank carrying liquid was highly affected by fluid sloshing and caused degradation of roll stability in comparison with vehicle carrying rigid cargo.

Keywords: *Liquid sloshing, tractor semi-trailer, vehicle dynamics, volume of fluid method (VOF), two phase flow, solid-fluid interaction*

1. Introduction

The stability and dynamic response characteristics of partially-filled tank vehicles are adversely influenced by movement of the liquid cargo within the tank which may cause risk to highway safety and environment, especially when dangerous liquid goods (toxic, flammable ...) are carried. Ervin et al reported[1] rollovers in nearly 75 percent of the total numbers of tank trucks highway accidents, while the rollover rate for conventional solid cargo vehicles were in the order of 54 percent.

Three factors in the sloshing cargo in a tanker could influence the lateral dynamics of the vehicle. First, inertia force because of liquid bulk motion causing roll moment on the vehicle and could be affected by tank geometry, tank fill level and fluid property. Second, induced force because of shift in the center of gravity of the fluid cargo that contributed to the roll moment on the vehicle. Third, resonance force because of proximity of sloshing frequency with steering excitation frequency or natural frequency of vehicle.

Fundamental slosh frequencies in a full size clean-bore tank occur in the 0.16-0.26 Hz range in the longitudinal mode and 0.56-0.74 Hz in lateral mode, depending upon fill volume and tank size [2]. Higher frequencies in lateral direction showed importance and complexity of consideration of slosh force and its interaction with vehicle dynamics in roll plane as induced in steer maneuvers. In the majority of fluid-vehicle coupled sloshing analysis, quasistatic approach [3-6] or mechanical analogy method has been applied [7-10] to calculate fluid slosh forces and moments.

Stranberg [11] studied roll stability of a tank vehicle under lane change and steady cornering maneuvers. He combined sloshing force from a laboratory model tank with a two DOF vehicle model. Ranganathan et al. [4] linked a kinetostatic roll-plane model of an articulated tank vehicle with a quasi-static sloshing model. Kang et al. [6] investigated directional stability of an articulated vehicle under combined turning and braking maneuvers, a quasistatic sloshing model of clean-bore tank coupled with the vehicle dynamics. Ranganathan et al. [12] evaluated directional responses of a tank under lateral acceleration, fluid sloshing modeled by a pendulum model which was moving in roll plane linked with a constant velocity vehicle model.

Quasi-static approach method, however is limited to fluid slosh in the steady state, and cannot be applied to study effects of baffles, particularly forces and moments arising from the transient slosh.

A few studies showed that magnitude of transient.

Fluid forces are larger than the quasi-static models [2, 13-14].Mechanical equivalent slosh methods generally are limited to clean-bore tanks and low amplitude sloshing. In these techniques, identification of the parameters in complicated tank shapes will also be challenging.

The effective and robust methods of solving transient fluid sloshing models are using the computational fluid dynamics (CFD) methods based on the Navier-Stokes solvers coupled with the Volume-of-Fluid (VOF) technique. These numerical approaches are known to be effective for simulating large-amplitude fluid slosh, under time-varying maneuver-induced accelerations [15-18]. Because of the complexity of coupling CFD methods with vehicle dynamics, these methods have been addressed in a few studies. Biglarbegian and zu [20] coupled a CFD code to an articulated clean-bore tank vehicle dynamics to study braking responses. Because of large computational demands, this study had been done for short duration of time (5 second). Guorong and Rakheja [13] studied straightline braking characteristics of a partly filled two-axle tank truck with baffles. They integrated a 3D fluid model with a Tank truck model.

In this paper, a tractor semi-trailer vehicle dynamics model has been integrated with a full scale three dimensional fluid model. Fluid sloshing model has been solved by Navier-Stokes equations coupled with volume of fluid (VOF) technique and the tractor semi-trailer vehicle's model. The dynamic response characteristics of tractor semi-trailer in different maneuvers have been considered and the effects of fluid sloshing on roll stability have been discussed in detail.

2. Vehicle Dynamic Simulation

The movement of liquid within a partly-filled tank caused by the lateral acceleration and roll motion of the semitrailer sprung mass depends on liquid fill volume, dynamics of the vehicle, tank shape and the type of vehicle's maneuver.

Commonly used tank's cross sections are circular, modified oval, elliptical or modified square. In this study a tank with circular cross section has been chosen.

The tractor is a two axles unit, typically used to tow a three-axle semi-trailer tanker. The tractor unit has a pair of single tires on the steer axle and a pair of twin tires on the drive axle. Semi-trailer has three axles and a pair of single tires which is fitted to each axle (as illustrated in Fig.1).

Tractor semi-trailer vehicle model has 5 DOF. The Tractor unit has freedom to side-slip, yaw and roll; while the semi-trailer has freedom to yaw and roll. The forward velocity is constant.

The equations representing the motions of the tractor unit are (see nomenclature in Appendix A):

$$m_1u_1(\dot{\beta}_1+\dot{\psi}_1)-m_{1s}(h_{1s}-h_{1r})\ddot{\phi}_1 = Y_{\beta 1}\beta_1+Y_{\dot{\psi}1}\dot{\psi}_1+Y_\delta\delta+F_{cy} \quad (1)$$

$$-I_{1xz}\ddot{\phi}_1+I_{1zz}\ddot{\psi}_1 = N_{\beta 1}\beta_1+N_{\dot{\psi}1}\dot{\psi}_1+N_\delta\delta-F_{cy}l_{1c} \quad (2)$$

$$I_{1x'x'}\ddot{\phi}_1-I_{1x'z'}\ddot{\psi}_1 = m_{1s}g(h_{1s}-h_{1r})\phi_1 + m_{1s}u_1(h_{1s}-h_{1r})(\dot{\beta}_1+\dot{\psi}_1)+ -(K_{1f}^*+K_{1r}^*)\phi_1-(C_{1f}+C_{1r})\dot{\phi}_1 K_{12}(\phi_2-\phi_1)-F_{cy}h_{1cr} \quad (3)$$

Roll motion of axles is neglected; the resultant effects of suspension and tire roll are given by:

$$\frac{1}{K_{1f}^*}=\frac{1}{K_{1f}}+\frac{1}{K_{1tf}},\ \frac{1}{K_{1r}^*}=\frac{1}{K_{1r}}+\frac{1}{K_{1tr}}$$

For semi-trailer unit the equations will be Sophisticated because of considering fluid forces and moments.

$$\bar{m}_2u_2(\dot{\beta}_2+\dot{\psi}_2)-\bar{m}_{2s}(h_{2s}-h_{2r})\ddot{\phi}_2 = Y_{\beta 2}\beta_2+Y_{\dot{\psi}2}\dot{\psi}_2-F_{cy}+F_y(t) \quad (4)$$

$$-\bar{I}_{2xz}\ddot{\phi}_2+\bar{I}_{2zz}\ddot{\psi}_2 = N_{\beta 2}\beta_2+N_{\dot{\psi}2}\dot{\psi}_2-F_{cy}l_{2c}+M_z(t) \quad (5)$$

$$\bar{I}_{2x'x'}\ddot{\phi}_2-\bar{I}_{2x'z'}\ddot{\psi}_2=\bar{m}_{2s}g(h_{2s}-h_{2r})\phi_2 +\bar{m}_{2s}u_2(h_{2s}-h_{2r})(\dot{\beta}_2+\dot{\psi}_2)-K_{2r}^*\phi_2 -C_{2r}\dot{\phi}_2-K_{12}(\phi_2-\phi_1)+F_{cy}h_{2cr}+M_{x'}(t) \quad (6)$$

The effect of the trailer suspension and tire roll in semitrailer unit is given by:

$$\frac{1}{K_{2r}^*}=\frac{1}{K_{2r}}+\frac{1}{K_{2tr}}$$

The kinematic constrain equation between the tractor and semi-trailer is obtained from Eq (7).

$$\dot{\beta}_2=\dot{\beta}_1+\frac{h_{1s}-h_{1c}}{u_1}\ddot{\phi}_1-\frac{h_{2s}-h_{2c}}{u_2}\ddot{\phi}_2 -\frac{l_{1c}}{u_1}\ddot{\psi}_1-\frac{l_{2c}}{u_2}\ddot{\psi}_2+\dot{\psi}_1-\dot{\psi}_2 \quad (7)$$

The response of above mentioned tractor semi-trailer model has been validated with the 9-DOF model [26].

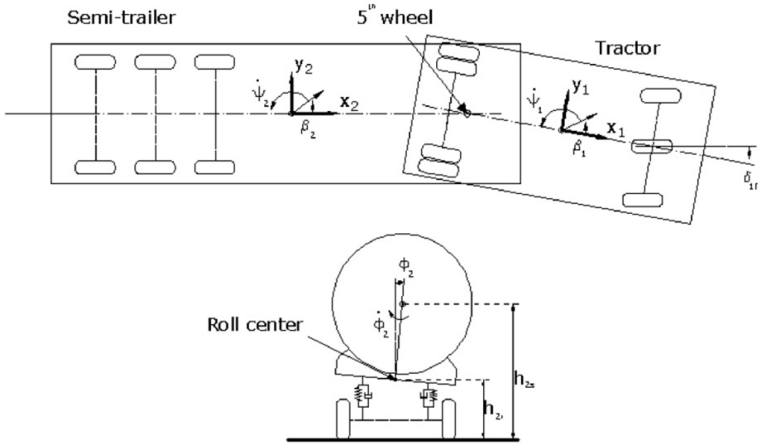

Fig1. Yaw and roll motion of tractor semi-trailer

Tire model:

The nonlinear variation of tire cornering stiffness with load z F has been considered as follows:

$$\frac{F_y}{\alpha} = c_1 \times F_z + c_2 \times F_z^2 \qquad (8)$$

C1, C2 are constants. This nonlinear model is suitable for lateral accelerations up to rollover point and widely used by vehicle simulations [22].

2.1 FLUID MODELING

Fluid movement within a partly filled tank can be considered as a two-phase flow, gas and liquid phases. Governing equations for movement of incompressible fluid are continuity and Navier-stokes mass conservation equations.

Continuity:

$$\nabla \cdot V = 0 \qquad (9)$$

Navier stokes:

$$\frac{\partial V}{\partial t} + \nabla \cdot (VV) = -\frac{1}{\rho}\nabla p + \frac{1}{\rho}\nabla \cdot \mu(\nabla V + (\nabla V)^T) + F_b \qquad (10)$$

Where V is the velocity vector of fluid relative to the global system of coordinates, p the pressure, ρ and μ the density and kinematic viscosity of the Liquid, respectively. F_b Represents body force (per unit volume) acting on the fluid. Zero-velocity Boundary conditions may be applied at the tank wall,

$$\frac{\partial V_n}{\partial n} = 0 \qquad (11)$$

Where V_n is normal velocity of the liquid at the boundary and n is the normal direction to the boundary. Tracking the free surface of the fluid is possible by solving volume fraction function f coupled with velocity V, volume of fluid method (VOF) [19].

$$\frac{\partial f}{\partial t} + \nabla \cdot (Vf) = 0 \qquad (12)$$

f is volume fraction, varying between zero to unit, unity for the cell fully occupied by fluid and zero for the cell occupied fully by gas.

The VOF technique, models two or more immiscible fluids by solving a single set of momentum equations. The density and viscosity for different phases are determined based on the following equations,

$$\rho = f_2\rho_2 + (1 - f_2)\rho_1 \qquad (13)$$

$$\mu = f_2\mu_2 + (1 - f_2)\mu_1 \qquad (14)$$

ρ_2, μ_2 and ρ_1, μ_1 indicate the densities and viscosities of air and water respectively. f_2 is the value of volume fraction of the liquid phase for a cell. The model has been established in FLUENT software.

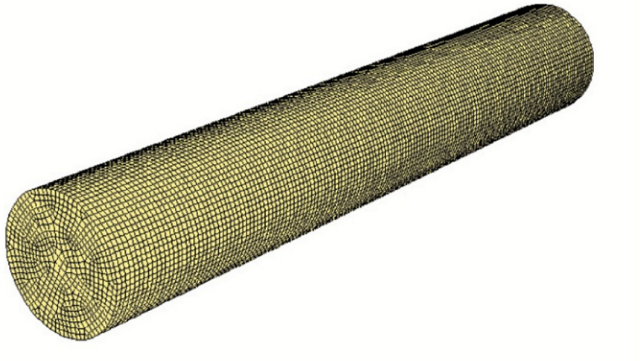

Fig2. Generated mesh for fluid dynamics analysis

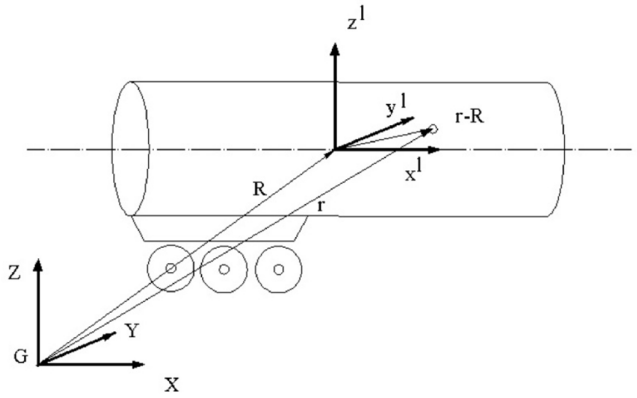

Fig3. Schematic diagram of the tank showing the moving and fixed coordinate frames

Fig 2 shows the mesh generation, 92040 hexahedral cells have been considered for fluid dynamics analysis. The governing equations sequentially are solved by using pressure correction and pressure-velocity coupling techniques. In every iteration, transient fluid force was calculated by integrating pressure over the wetted tank wall and moment was calculated by cross productions of position vector $\bar{r}_i$ and force vector F_i all over wetted faces cell.

$$F(t) = \sum_{Q} P_i \cdot A_i \quad (15)$$

$$M(t) = \sum_{Q} \bar{r}_i \times F_i \quad (16)$$

P_i is pressure and A_i is area vector of the ith wall cell. Q showing wetted face on tank wall and $\bar{r}_i$ is position vector of wall cell from tank coordinate system.

2.2 Coupling the fluid sloshing and vehicle model

The body coordinates $(x, y, z)^l$ are attached to the center of the tank. The tank rotates with angular velocity vector, Ω, and translational velocity vector, U , with respect to the inertial frame X, Y, Z of origin G .

The external force is the sum of the gravitational force, transitional, and rotational inertia forces, that is

$$F_b = g - \frac{dU}{dt} - \frac{d\Omega}{dt} \times (r - R) - 2\Omega \times \frac{d(r-R)}{dt} - \Omega \times [\Omega \times (r - R)] \quad (17)$$

Where r and R are position vectors of a fluid particle and the tank center with respect to the inertial fixed frame. The above formulation has been used to calculate fluid external force in Navier-Stokes equation (9).

The vehicle model has been modeled in inertia coordinate system which origins are located on sprung mass center of gravity of tractor and semi-trailer and fluid model developed in the tank coordinate system $(x, y, z)^l$ and its origin is located on

the geometric center of tank. Vehicle model initially solved for static fluid condition. In the first step, the steer input applied to vehicle model and vehicle responses would be computed in the (x, y, z) coordinate and by transforming the results to tank coordinate $(x, y, z)^l$ the body force could be calculated (13). By knowing the body force, the fluid subsystem could be solved individually; the output of the sloshing model would be resultant fluid forces and moments in $(x, y, z)^l$ coordinate. Next, transformation of forces and moments from $(x, y, z)^l$ to (x, y, z) would be done and results would be used as an external force on the vehicle dynamic model Therefore, in every time step, two subsystems (vehicle dynamics and fluid sloshing models) would be solved simultaneously. The above mentioned procedure will be continued subsequently until the end of simulation time (Fig 5). For model convergence, time step must be considered so small.

The vehicle model is numerically solved by using the fourth-order Runge-Kutta method while the CFD analysis uses first-order discritization in the space and time domain.

3. . Results and discussion

Tractor joined to a three-axle Semi-trailer by fifth wheel coupling. The tractor and semi-trailer parameters are from experimental vehicle (APPENDIX B) [21]. The simulation has been done for 50 % filled tank vehicle carrying water of density $998\ kg/m^3$.

Steady state turning

The response behavior of five-axle vehicle, initially evaluated under steady input of 2 degree (Fig 5) at constant speed of $60\ km/hr$.

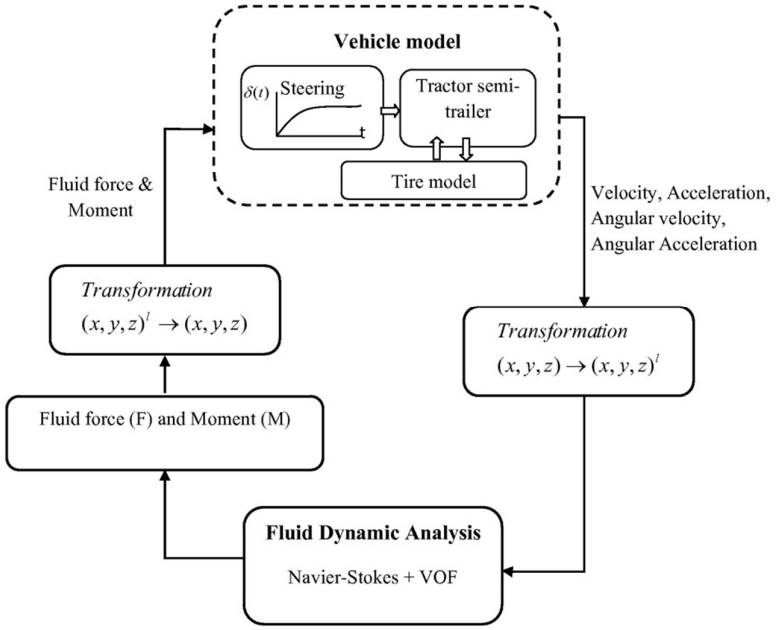

Fig4. Simulation procedure of fluid dynamics coupled with vehicle model

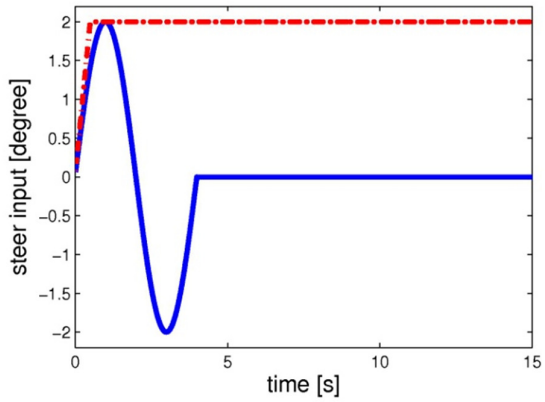

Fig5. Steer input for two maneuvers; - - . Steady steer, __ lane-change steer input for two maneuvers; - - . steady steer, __ lane-change

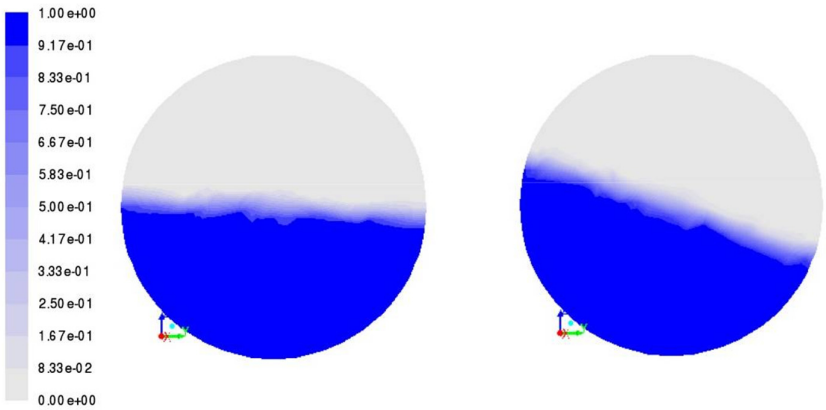

Fig6. Fluid surface at x=0 t= 1, t= 2.25 second, steady state turning

Fig 6 illustrates fluid and fluid surface position at t=1 and t=2.25 second. As expected, at t=1 second, fluid surface inclination is small but it grows over the time. At t=2.25 second, surface inclination increases with considerable slope.

Fig 7 illustrates the steady steer response of coupled vehicle-tank (solid line) and equivalent rigid cargo (dash line). It shows tractor and semi-trailer main responses, variation in the roll angle ϕ and yaw rate $\dot{\psi}$ .The simulations have also been performed for an equivalent rigid cargo and the responses are compared with partly filled tank. The roll angle of tractor and trailer are considerably greater than the equivalent rigid cargo tank.

In comparison with equivalent rigid cargo, the roll angle's of semi-trailer tank carrying liquid shows 70% increment in peak condition and 65% increment in steady state condition. The roll angle of tractor and trailer tend to oscillate about steady state values.

Because of permanent shift of fluid inside the tank in steady steer input (constant radius), the magnitude of roll angle have shifted about the equivalent of rigid cargo. The magnitudes of yaw rate of tractor and trailer are slightly higher than the equivalent rigid cargo but the responses approach steady state value of the equivalent rigid cargo.

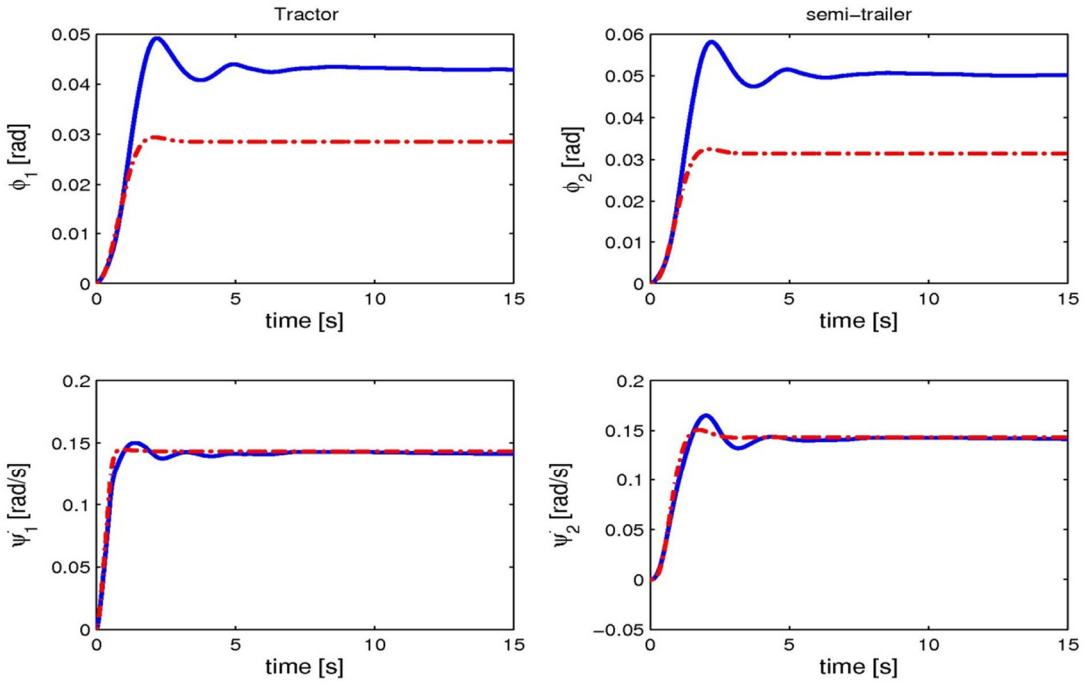

Fig7. The transient responses of tractor semi-trailer; —— fluid cargo; - - - equivalent rigid cargo

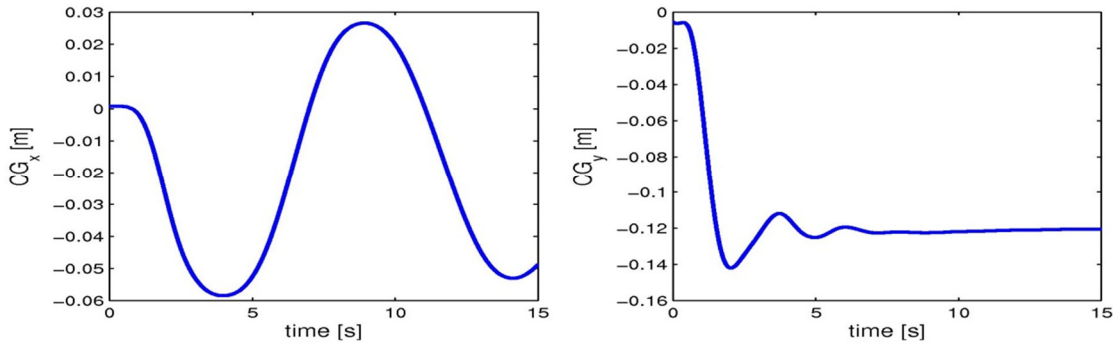

Fig8. Fluid's center of gravity coordinates (longitudinal and lateral)

Fig 8 illustrates the fluid center of gravity's movements in longitudinal and lateral directions. Changes of center of gravity of fluid in lateral direction are higher than longitudinal direction and its oscillatory behavior is because of fluid movement inside the tank but its value approaches to a steady state negative value (as expected).

Lower frequency in longitudinal direction is related to the higher ratio of the length of tank to its diameter; however the frequency could be influenced by vehicle's dynamics and input steer frequency [13].

Fig 9 illustrates resultant fluid force on the body of the tank. The fluid forces are calculated base on the formula (15). Fluid force in longitudinal direction has oscillatory behavior but approaches to steady state value.

Since the induced acceleration by the steady steer maneuver in lateral direction is higher than the longitudinal direction, force in lateral direction is greater than longitudinal direction.

The magnitude of force in lateral direction has the same oscillatory behavior and its magnitude is negative during the simulation time. Force in

horizontal direction is mostly affected by gravitational force and its magnitude oscillates around the weight of fluid cargo.

Fig 10 illustrates tractor and trailer's center of gravity accelerations for fluid cargo (solid line) and equivalent rigid cargo (dash line). The acceleration of semi-trailer is slightly higher than tractor's. The peak accelerations (tractor and trailer) for fluid cargo are slightly higher than the equivalent rigid cargo and their oscillatory behaviors diminish and converge to a steady state value as the equivalent rigid cargo.

The vehicle's roll over characteristics is described in term of dynamic load factor (DLF). The dynamic vertical load factor is defined as the ratio of the vertical load on the left or right wheel of a given axle to the static load on that axle, Where F_{zr} and F_{zl} are vertical loads on the right and left wheels of an axle. During a turning maneuver, the dynamic load factor is initially one and may approaches to zero when the tires lose contact with the road.

$$DLF_r = \frac{2F_{zr}}{F_{zr}+F_{zl}} \quad , \quad DLF_l = \frac{2F_{zl}}{F_{zr}+F_{zl}} \tag{18}$$

The dynamic vertical load factor of the other wheel in this situation will attain the maximum value of two. The rearmost track is the most susceptible to lose its contact [6]. The roll dynamics of the vehicle combination as a whole, however, can be effectively evaluated in terms of the dynamic load transfer ratio (LTR), which is defined as the instantaneous ratio of the absolute value of the difference between the sum of the right wheel loads and that of the left wheel loads, to the sum of all the wheel loads, and is expressed as:

$$LTR = \sum_{j=1}^{N} \frac{\left|F_{zrj} - F_{zlj}\right|}{F_{zrj} + F_{zlj}} \tag{19}$$

Where N is the number of axles. For vehicles with trailer units that are decoupled in roll, load transfer ratio calculations apply only within the independent units. The front steering axle is usually excluded from the calculations because of its relatively high roll compliance. The LTR assumes an initial value of zero and reaches unity when the wheels on the inside of the turn lift off the ground.

Fig. 11 illustrates dynamic load factor characteristics for rearmost axle and load transfer ration for fluid cargo and equivalent rigid cargo. This figure shows that the fluid cargo DLF for right wheel is lower than the equivalent rigid cargo (45% lower in the peak and 30% in steady-state conditions). It also shows that the trailer with fluid cargo is most susceptible to lose tires contact and overturning.

These results completely coincide with the experiences that articulated vehicle which carry fluid are most susceptible to lose their roll stability in comparison with the vehicle carrying rigid cargo[11].

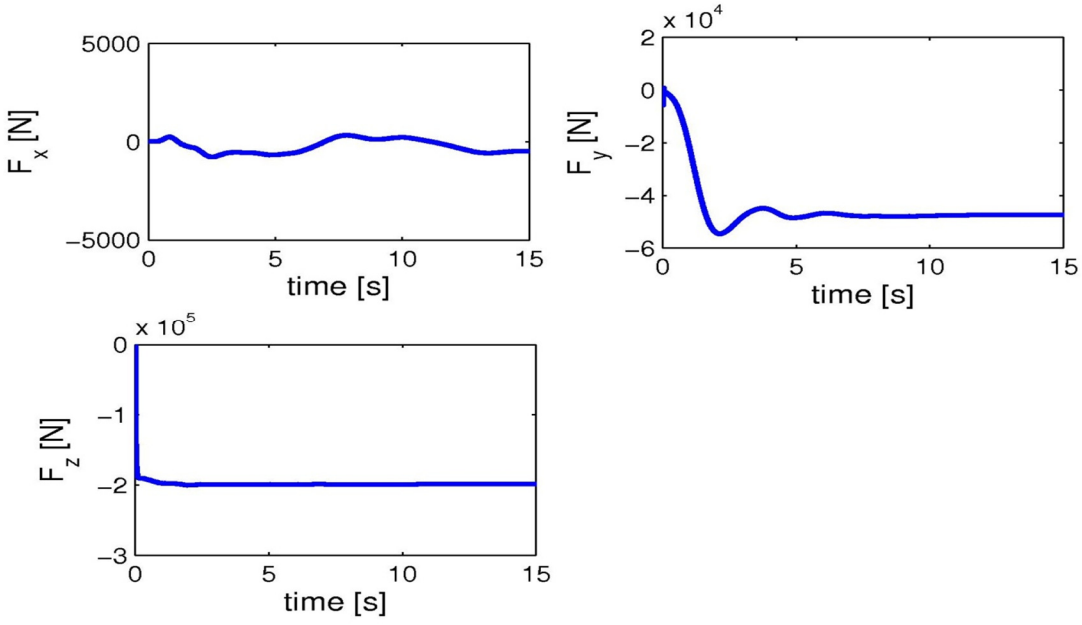

Fig9. Resulting fluid force on the body of the tank

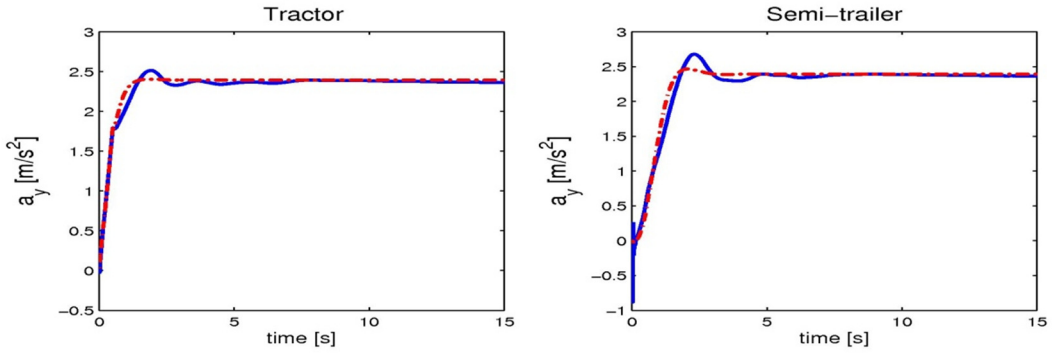

Fig10. Center of gravity accelerations; _____ fluid cargo, - - - - - equivalent rigid cargo

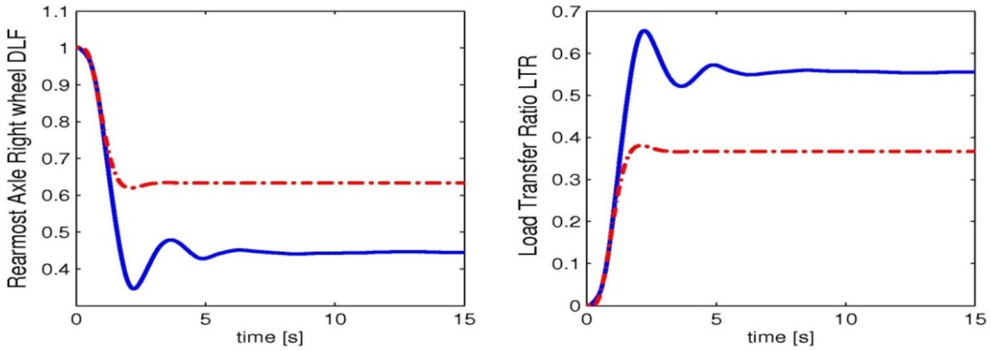

Fig11. Rearmost Axle Right wheel Dynamic Load Factor and Load Transfer Ratio; —— fluid cargo, - - - -equivalent rigid cargo

Transient steer input

The directional and roll response characteristics of partly filled articulated vehicle were investigated under lane-change maneuver (Fig. 5). The analyses were performed for 50% filled volume tank.

Fig 12 illustrates main response characteristics including roll angle ϕ and yaw rate $\dot{\psi}$ of tractor and trailer. The simulation has also been performed for the equivalent rigid cargo (dash line) and the responses have been compared. Roll angles of tractor and trailer have mostly been affected by the fluid movement inside the tank. In comparison with equivalent rigid cargo, tractor roll angle shows the 60% increment in its first peak and 80% increment in the second peak. The same result can be concluded for trailer's roll angle. Yaw rate of tractor and trailer are slightly higher than equivalent load especially in second peak t=3.9s.

Fig 13 illustrates fluid cargo's center of gravity coordinates in longitudinal and lateral directions. Most changes of center of gravity of fluid are in the lateral direction and its oscillatory behavior is related to the fluid movement inside the tank but its value approaches to a steady state value of zero.

It means that after a lane change maneuver in steady state condition, fluid's center of gravity will turn back to its initial state. Center of gravity in longitudinal direction has lower magnitude and frequency.

Fig 14 illustrates resultant fluid force on the body of the tank. Fluid force in longitudinal direction has oscillatory behavior and its magnitude is small in comparison with lateral direction. Force in lateral direction has oscillatory behavior. The sign of lateral force is negative until third second but it turns to positive (as expected) because of changes in sign of steer angle in the second half cycle of lane change maneuver and also fluid movement inside the tanker.

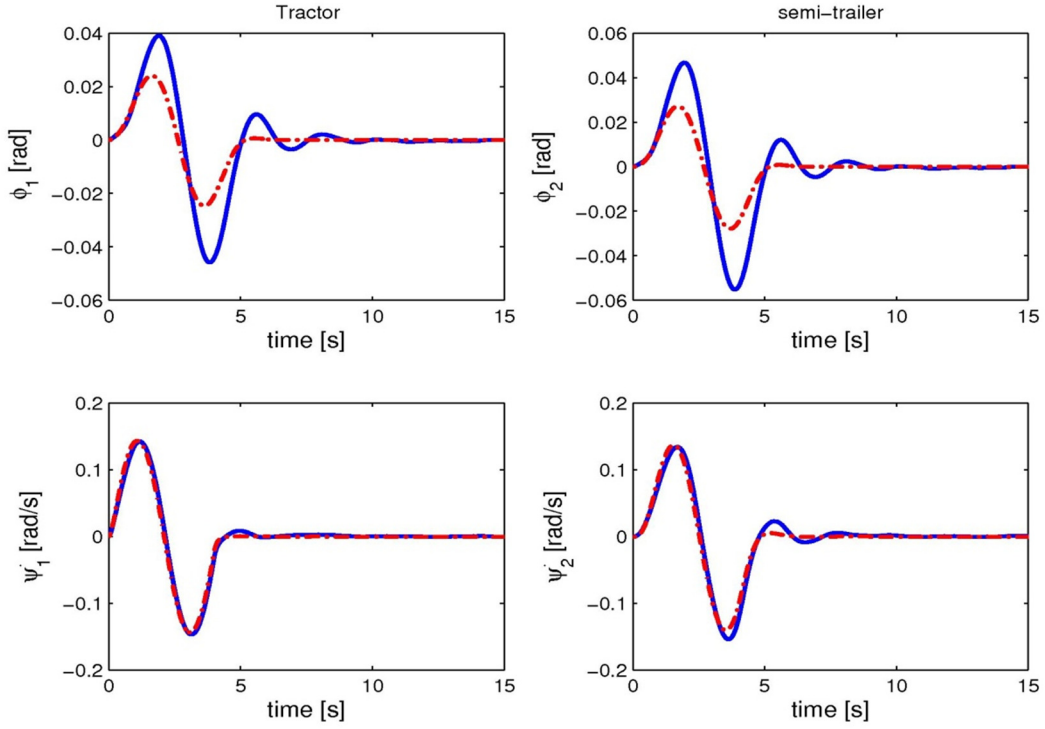

Fig12. The transient responses of tractor semi-trailer; —- fluid cargo, - - - - equivalent rigid cargo

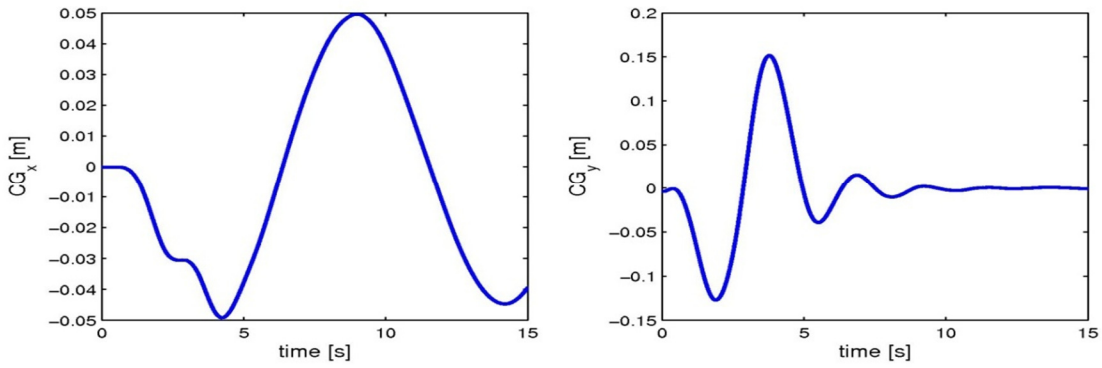

Fig13. Fluid's center of gravity coordinates (longitudinal and lateral)

Force in horizontal direction is mostly affected by gravitational force and its magnitude in steady condition is close to the weight of fluid cargo.

Fig 15 illustrates tractor and trailer center of gravity accelerations for fluid cargo (solid line) and equivalent rigid cargo (dash line). The peak acceleration of fluid cargo is little smaller than the equivalent rigid cargo and its oscillatory behavior diminishes after 15 second and it converges to a steady state value of zero as the equivalent rigid cargo accelerations .Fig 16 illustrates dynamic load factor characteristics (DLF) for rearmost axle right wheel and load transfer ratio (LTR), for fluid cargo and equivalent rigid cargo. This figure shows that the fluid cargo's minimum DLF of fluid cargo for right wheel is lower than the equivalent rigid cargo 40% in the first peak (2 second)). Minimum DLF of fluid cargo for left wheel is 80% lower than rigid cargo in second peak (4 second)). It shows that the trailers with fluid cargo are most

susceptible to lose tires contact and overturning. It also shows that in the second half of cycle of the lane change maneuver, load transferring to right wheel is serious and probability of losing tire contact for left wheel will increase dramatically.

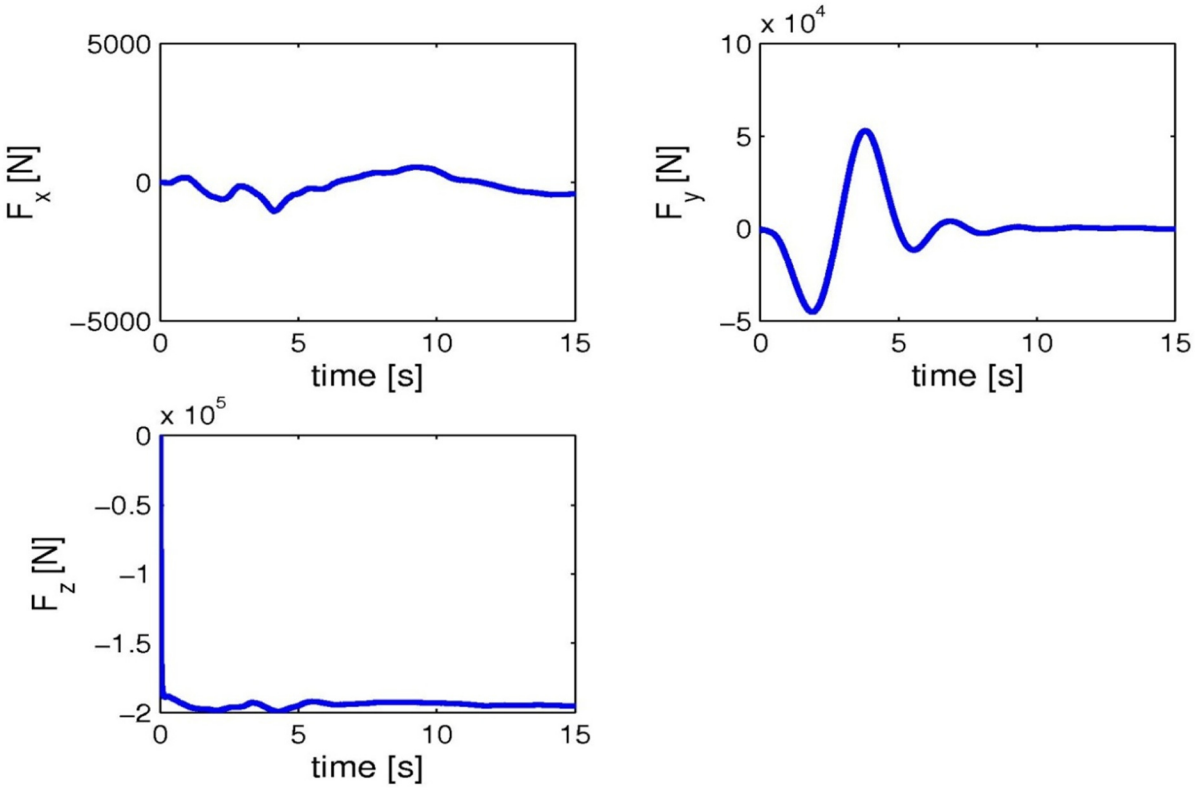

Fig14. Resulting fluid force on the body of the tank

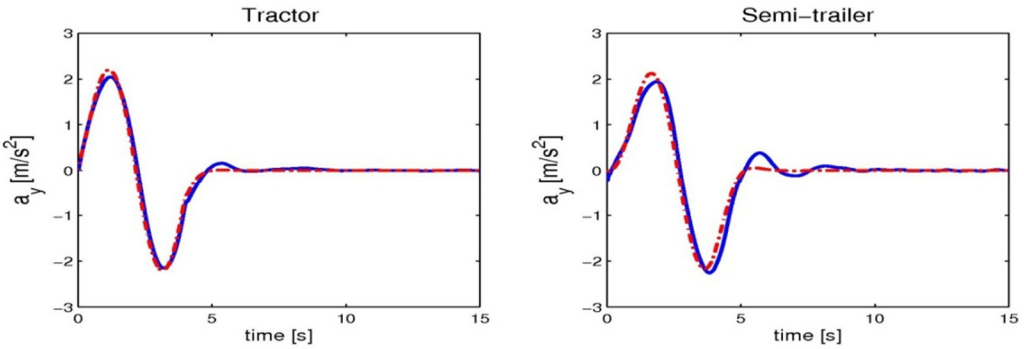

Fig15. Center of gravity accelerations; —— fluid cargo, - - - - equivalent rigid cargo

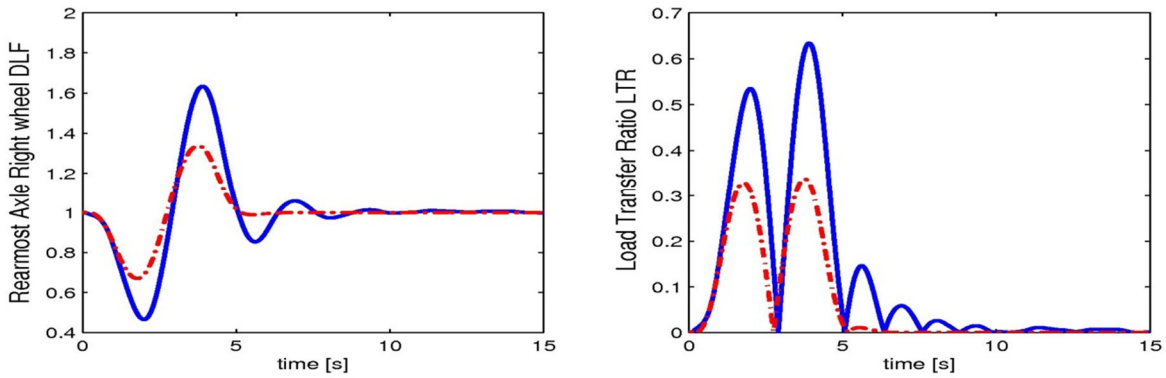

Fig16. Rearmost Axle's right wheel Dynamic Load Factor and Load Transfer Ratio; —— fluid cargo, - - - -equivalent rigid cargo

Conclusion

In this article, a complete dynamic model of a tractor semi-trailer vehicle is modeled and coupled to a 3D full scale tank's fluid dynamics to study the dynamic behaviors of the vehicle subject to liquid slosh loads during steady and transient steering inputs. The effects of fluid slosh of a partly filled tank were considered by fluid forces and moments derived from computational fluid dynamic model linked with VOF technique. The steady state turning and lane-change maneuvers have been performed and dynamic responses compared with equivalent rigid cargo. The results revealed that the vehicle responses are greatly affected by fluid slosh. The roll angles highly affected by fluid movement but the yaw rate changes would be small.

Roll stability of vehicle is also affected by fluid movement inside the tank, describing by dynamic load factor and load transfer ratio. The results showed the fluid sloshing model interaction with the vehicle dynamic increases probability of roll over occurrence. This probability is higher in the lane change maneuver (transient steer); especially in the second half of lane-change maneuver. This means that in a lane-change maneuver, roll over occurs in the time that the driver doesn't expect.

References

[1]. Ervin, R. D., Barnes, M. and Wolfe, A. Liquid cargo shifting and the stability of cargo tank trucks. Report UMTRI-85-35/1, University of Michigan Transportation level). Research Institute, 1985.

[2]. Modaressi-Tehrani, K., Rakheja, S. and Stiharu, I. Three dimensional analysis of transient slosh within a partly-filled tank equipped with baffles, Vehicle Syst. Dyn, 2007, 45(6), 525-548.

[3]. Rakheja, S., Sankar, S. and Ranganathan, R. Roll plane analysis of articulated tank vehicles during steady turning, Vehicle Syst. Dyn., 1988, 17, 81-104.

[4]. Ranganathan, R., Rakheja, S. and Sankar, S. Kineto-static roll plane analysis of articulated tank vehicles with arbitrary tank geometry, Int. J. of Vehicle Design, 1989, 10(1), 89-111.

[5]. Rakheja, S. and Ranganathan, R. Estimation of the Rollover Threshold of Heavy Vehicles Carrying Liquid Cargo: A Simplified Approach. Heavy Vehicle Systems, Int. J. of Vehicle Design, 1(1), 1993, 79-98.

[6]. Kang, X., Rakheja, S. and Stiharu. I. Cargo load shift and its influence on tank vehicle dynamics under braking and turning, Int. J. Heavy Vehicle Syst, 2002, 9(3), 173 -203.

[7]. Dodge, F. T. Analytical representation of lateral sloshing by equivalent mechanical models, Report, NASA SP-106, 1996.

[8]. Salem, M. I., Mucino, V. H., Saunders, E. and Gautam, M. Lateral sloshing in partially filled elliptical tanker trucks using a trammel pendulum, Int J. Heavy Vehicle Syst, 2009, 16(1-2), 207-224.

[9]. Solaas, F. and Faltinsen, O. M. Combined numerical and analytical solution for sloshing in two-dimensional tanks of general shape, J. Ship Res., 1997, 41, 118-129.

[10]. Salem, M. I., Mucino, V., Aquaro, M. and Gautam, M. Review of parameters affecting stability of partially filled heavy duty tankers, Proc. SAE Int. Truck \& Bus Meet Expo, Detroit, MI, November 1999, paper no. 1999-01-3709.

[11]. Strandberg, L. Lateral Stability of Road Tankers. VTI Rapport No. 138A, Sweden, Vol. 1, 1978.

[12]. Ranganathan, R., Ying, Y. and Miles, J. B. Analysis of fluid slosh in partially filled tanks and their impact on the directional response of tank vehicles, 1993, SAE paper no.932942, pp. 39-45.

[13]. Guorong, Y. and Rakheja, S. Straight-line braking dynamic analysis of a partly-filled baffled and unbaffled tank truck, I. Mech. E., J. Auto Eng., 2009, 223, 11-26.

[14]. Romero, J. A., Hildebrand, R., Martinez, M., Ramirez, O. and J. M. Fortanell. Natural sloshing frequencies of liquid cargo in road tankers, Int. J. Heavy Vehicle Syst., 2005, 12(2), 121-138.

[15]. Hirt, C. W., Nicholas, B. D. and Pomeroy, N. C. SOLA- a numerical solution algorithm for transient fluid flows. Report LA-5852, Los Alamos Scientific Laboratory, Los Alamos, New Mexico, USA, 1975.

[16]. Hirt, C. W., Nicholas, B. D. Volume of fluid (VOF) method for the dynamics of free boundaries, J. Comput Phys., 1981, 39(1), 201-225.

[17]. Issa, R. I. Solution of implicitly discretized fluid flow equations by operator splitting, J. Comput. Phys., 1986, 62, 40-65.

[18]. [18]- Partom, I. S. Application of the VOF method to the sloshing of a fluid in a partially filled cylindrical container, Int. J. Numer Methods Fluids, 1987, 7(6), 535-550.

[19]. FLUENT 6.2.16 Documentation, User's Guide, Chapter 24, General Multiphase models, 2005.

[20]. Biglarbegian, M. and Zu, J. W. Tractor-semitrailer model for vehicles carrying liquids. Veh. System Dynamics, 2006, 44, 871-885

[21]. Sampson, D. J. M. Active Roll Control of Articulated Heavy Vehicles. PhD. thesis, University of Cambridge, Cambridge, UK, 2000.

[22]. Fancher, P. S., Ervin, R. D., Winkler, C. B. and Gillespie, T. D. A fact book of the mechanical properties of the components for single-unit and articulated heavy trucks. Technical Report UMTRI-86-12, University of Michigan Transportation Research Institute, Ann Arbor, MI, USA, 1986.

APPENDIX A

Nomenclature

A_i : area vector of ith wall

a_{y2} :lateral acceleration of COG of whole trailer mass

a^* :longitudinal distance to axle, measured backward from front axle or from front articulation point.

b^* : longitudinal distance to articulation point, measured backwards from front axle.

c_1, c_2 : tyre cornering stiffness coefficients

$C_{if/r}$: roll damping of suspension (front/rear)

$C\alpha_{if/r}$: cornering stiffness of tyres on front/rear axle (N/rad)

f : value of volume fraction

F_i :force vector of i th wall cell

F_b :body force per unit value of fluid

F_{cy} :lateral component of directional forces at articulation point (articulation angle is small)

F_z : vertical tyre force

$F(t)$: fluid force on the body of the tank

g : acceleration due to gravity

h_{ic} : height of articulation point, measured upwards from ground

h_{ir} :height of roll centre of sprung mass, measured upwards from ground

h_{is} :height of centre of sprung mass, measured upwards from ground

h_u :height of center of unsprung mass, measured upward from ground

I_{ixx} :roll moment of inertia of sprung mass, measured about sprung centre of mass

$I_{ix'x'}$:roll moment of inertia of sprung mass, measured about roll centre of vehicle unit

I_{ixz} :yaw-roll product of inertia of sprung mass, measured about sprung centre of mass

$I_{ix'z'}$:yaw-roll product of inertia of sprung mass, measured about roll centre of vehicle unit

I_{izz} :yaw moment of inertia of sprung mass, measured about sprung centre of mass

$\bar{I}_{ixx}$:roll moment of inertia of unladen sprung mass, measured about sprung centre of mass

$\bar{I}_{ix'x'}$: roll moment of inertia of unladen sprung mass, measured about roll centre of vehicle unit

$\bar{I}_{ixz}$:yaw-roll product of inertia of unladen sprung mass, measured about sprung centre of mass

$\bar{I}_{ix'z'}$: yaw-roll product of inertia of unladen sprung mass, measured about roll centre of vehicle unit

$\bar{I}_{izz}$: yaw moment of inertia of unladen sprung mass, measured about sprung centre of mass

K_{12} : roll stiffness of articulation point

$K_{if/r}$: roll stiffness of suspension (front/rear)

$K^*_{if/r}$:adjusted roll stiffness of suspension (front/rear)

$K_{itf/r}$:roll stiffness of tyre (front/rear)

$l_{if/r}$:distance between the sprung mass COG and axle

$M(t)$:fluid moment, measured about geometric center of tank

$M_{x'}(t)$: fluid moment, measured about roll center of vehicle unit

m_i :total mass of tractor or semi-trailer

m_{is} : sprung mass of tractor or semi-trailer

$\bar{m}_i$: total unladen mass of tractor or semi-trailer

$\bar{m}_{is}$: unladen sprung mass of tractor or semi-trailer

$N_{\beta i}$: $\frac{\partial M_z}{\partial \beta} = \sum_j l_{i.j} C\alpha_{ij} =$ partial derivative of net tyre yaw moment with respect to side-slip angle

$N_{\delta i}$: $\frac{\partial M_z}{\partial \delta_i} = -l_{i.f/r} C\alpha_{if/r} =$ partial derivative of net tyre yaw moment with respect to steer angle

$N_{\dot{\psi} i}$: $\frac{\partial M_z}{\partial \dot{\psi}_i} = \sum_j \frac{-l^2_{i.j} C\alpha_{ij}}{u_i} =$ partial derivative of net tyre yaw moment with respect to yaw rate

$\bar{r}_i$:position vector of wall cell from tank coordinate

U :transitional velocity vector

u_i :longitudinal velocity of tractor or semi-trailer

V : velocity vector

W : axle weight

$\bar{W}$: unladen axle weight(%50 filled volume)

$Y_{\beta i}$: $\frac{\partial F_y}{\partial \beta_i} = \sum_j C\alpha_{if/r} =$ partial derivative of net tyre lateral force with respect to side-slip angle

$Y_{\delta i}$: $\frac{\partial F_y}{\partial \delta_i} = -C\alpha_{if/r} =$ partial derivative of net tyre lateral force with respect to steer angle

$Y_{\psi i}$: $\frac{\partial F_y}{\partial \dot{\psi}_i} = \sum_j \frac{l_{i.j} C\alpha_{ij}}{u_i}$ = partial derivative of net tyre lateral force with respect to yaw rate

α_i :tire slip angle

β_i :side-slip angle of vehicle body

δ : steering angle of vehicle axles

ϕ_i :absolute roll angle of sprung mass

ψ_i :yaw angle of vehicle body

ρ :density

μ : viscosity

Ω :angular velocity vector